

The small flaw tolerance of a brittle structure

E. SMITH

*Manchester University-UMIST Materials Science Centre, Grosvenor Street,
Manchester M1 7HS, UK*

On the basis that the dominant source of the maximum load-size effect for an uncracked brittle structure is deterministic, it can be associated with the formation of a damage (fracture process) zone at a free surface. By modelling this damage in terms of the cohesive zone description, and associating the maximum load with the attainment (at the free surface) of an elastically calculated effective tensile failure stress, earlier work has shown that the effective stress is critically dependent on the applied loading-included stress gradient beneath the surface, with the effective failure stress increasing with the steepness of the stress gradient. The earlier considerations have been extended in the present work to assess the effect of a small surface flaw (crack) on the effective failure stress, and to show how the small flaw tolerance, as manifested by the reduction in effective failure stress, depends on the stress gradient, flaw depth and material fracture parameters. © 1998 Kluwer Academic Publishers

1. Introduction

Uncracked brittle structures or laboratory test specimens exhibit a maximum load-size effect, which is conveniently illustrated by considering the case of an uncracked bent beam specimen for which the maximum stress occurs at the tensile surface. Assuming elastic behaviour and with the beam depth and thickness being, respectively, w , and B , the bending moment, M , is equal to $Bw^2\sigma_s/6$, where σ_s is the tensile stress at the surface. Experiments, for example with unreinforced concrete beams, have shown that the maximum moment, M_m , that a beam is able to sustain is $Bw^2\sigma_m/6$, with $\sigma_s = \sigma_m$ and where σ_m is the effective failure stress and increases as the beam depth, w , decreases [1, 2].

As recently emphasised by Li and Bazant [3], the underlying cause of the size effect for brittle and quasi-brittle materials such as concrete, rocks, ceramics and ceramic-based composites, stems from the observation that they exhibit damage (fracture process) zones which are able to develop and grow prior to the attainment of maximum load. The dominant source of the size effect is, therefore, seemingly deterministic, and is related to the manner in which a damage zone develops. Against this background, the behaviour of a damage zone emanating from a planar surface has been modelled [4] and, using an infinitesimally thin cohesive zone description, it was shown how the effective failure stress increases with the steepness of the applied loading-induced stress gradient beneath the surface, thereby providing a ready explanation as to why the effective failure stress for an uncracked bent beam increases as the beam depth decreases. Subsequent work [5] has extended the considerations to the case where failure arises as a result of the

formation of a damage zone at the surface of a blunt stress concentration, and has shown how the effective failure stress increases with the severity of the stress concentration, i.e. as the root radius decreases. The present work assesses the effect of a small surface flaw on the effective failure stress, and shows how the small flaw tolerance, as manifested by the reduction in effective failure stress, depends on the stress gradient, flaw depth and material fracture properties.

2. Outline of the cohesive zone description of a damage zone

Following the pattern adopted in the earlier work [4, 5], we represent a damage zone by a cohesive zone. Thus, a single, infinitesimally thin, two-dimensional cohesive zone forms ahead of a surface (or crack tip in the context of the present work's considerations) as the applied load or stress increases, the zone spreading into the interior of the structure. The zone can, in general, be characterized by a material-specific relation between the tensile stress p , and the relative displacement, v , between the zone faces, with p being a maximum, p_c , at the leading edge of the cohesive zone. The zone is said to be fully developed when the stress falls to zero at the trailing edge of the zone, i.e. at the crack tip, a situation that is assumed to be attained when the displacement attains a critical value, v_c . With a general $p-v$ cohesive zone behaviour, the maximum load or stress, and thereby failure in a load-control situation, is attained prior to the cohesive zone's full development. However, in order to simplify the considerations, and following the pattern adopted in the earlier work, it will be assumed here that the stress p , within the cohesive zone remains constant at the

value, p_c , until the displacement, v , attains the critical value, v_c , when the stress is assumed to fall abruptly from p_c to zero. This is the classic Dugdale–Bilby–Cottrell–Swinden (DBCS) representation [6, 7] that is often used to model stress-relaxation phenomena. With this specific zone behaviour, the attainment of maximum load or stress, and thereby failure, is associated with the full development of the cohesive zone.

3. Cohesive zone formation at a crack in a planar surface

Consider the two-dimensional situation where there is a crack of depth c in the planar surface of a semi-infinite solid (Fig. 1); there is a cohesive zone, within which the tensile stress is p_c , emanating from the crack tip, this zone extending to a distance a from the planar surface. It is assumed that the tensile “driving” stress, p_{22} , along the plane $X_2 = 0$ in the absence of the cohesive zone is

$$\sigma(x) = \sigma_L \left(1 - \frac{x}{h}\right) \quad (1)$$

where x is measured from $X_1 = 0$ along the X_1 axis; σ_L is the stress at the surface, and h is a length parameter which is a measure of the stress gradient. The isolated crack (length $2c$)–infinite body solution will be used as an approximate solution for our situation, by making a cut along the symmetry plane $X_1 = 0$, a procedure which is exact for the analogous Mode III problem.

For the stress to be finite ($= p_c$) at the in-board extremity of the cohesive zone, standard results [8] give

$$\frac{\sigma_L}{p_c} \left(\frac{\pi}{2} - \frac{a}{h}\right) = \cos^{-1} \left(\frac{c}{a}\right) \quad (2)$$

Furthermore, standard results [8] give the relative displacement $\Phi(c)$ of the cohesive zone faces at the crack tip as

$$\begin{aligned} \Phi(c) = & \frac{4\sigma}{E_0} (a^2 - c^2)^{1/2} \\ & - \frac{4\sigma a^2}{\pi E_0 h} \left[\left(1 - \frac{c^2}{a^2}\right)^{1/2} + \frac{c^2}{a^2} \cosh^{-1} \left(\frac{a}{c}\right) \right] \\ & - \frac{8p_c}{\pi E_0} (a^2 - c^2)^{1/2} \cos^{-1} \frac{c}{a} + \frac{8p_c c}{\pi E_0} \ln \left(\frac{a}{c}\right) \quad (3) \end{aligned}$$

where $E_0 = E/(1 - \nu^2)$, E being Young’s modulus and ν being Poisson’s ratio. Equations 2 and 3 allow us to obtain the effective failure stress σ_m by setting $\sigma_L = \sigma_m$ and $\Phi(c) = v_c$. Thus with $\chi = v_c E_0 / 2\pi p_c h$, $x = c/h$, $u = a/h$ and $y = \sigma_m / p_c$, we see that σ_m is given by the relation

$$y = \frac{\sigma_m}{p_c} = \cos^{-1}(x/u) \left/ \left(\frac{\pi}{2} - u\right) \right. \quad (4)$$

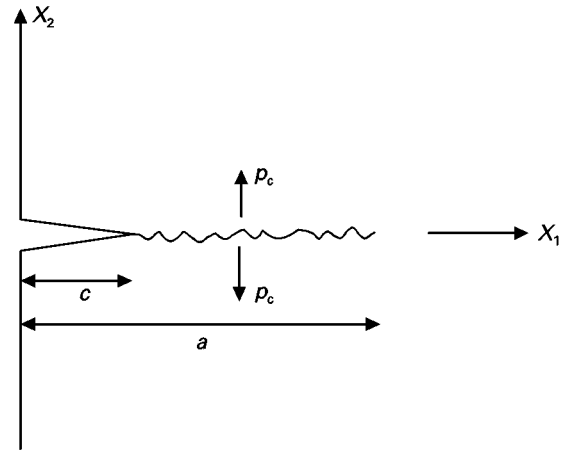


Figure 1 The model of a cohesive zone emanating from the tip of a crack in the planar surface of a semi-infinite solid.

with

$$\begin{aligned} \frac{\pi^2 \chi}{4} = & \left[\frac{u}{\pi} (u^2 - x^2)^{1/2} \cos^{-1}(x/u) \left/ \left(1 - \frac{2u}{\pi}\right) \right. \right] \\ & - x \ln \left(\frac{x}{u}\right) - \frac{x^2}{\pi} (\cos^{-1}(x/u) \cosh^{-1}(u/x)) \left/ \left(1 - \frac{2u}{\pi}\right) \right. \quad (5) \end{aligned}$$

We are concerned with the effect of a small crack in a stress gradient, and how this reduces the effective failure stress below the value appropriate to the case where there is no crack. Thus we are interested in the situation where χ is finite and where $x = c/h$ is small. Now, in the limiting case where there is no crack, i.e. $x = 0$, let $u = u_0$ and $y = y_0$, whereupon Equations 4 and 5 give, for this special case

$$u_0 = \frac{\pi}{2} [(2\chi + \chi^2)^{1/2} - \chi] \quad (6)$$

$$y_0 = 1 + \chi + (2\chi + \chi^2)^{1/2} \quad (7)$$

these expressions being in accord with those obtained in the earlier work [4].

Now when x is small and χ is finite, let $u = u_0 + \Delta u_0$ and $y = y_0 + \Delta y_0$ where Δu_0 and Δy_0 are both small. Then, to the first order in small quantities, Equation 4 gives

$$\Delta y_0 = \frac{2}{\pi} \left[\left\{ \frac{\Delta u_0}{\left(1 - \frac{2u_0}{\pi}\right)} \right\} - \frac{x}{u_0} \right] \left/ \left(1 - \frac{2u_0}{\pi}\right) \right. \quad (8)$$

while Equation 5 gives, again to the first order in small quantities

$$\Delta u_0 = \left[\frac{x}{u_0} \left(1 - \frac{2u_0}{\pi}\right) \left/ \left(1 - \frac{u_0}{\pi}\right) \right. \right] \left[\frac{u_0}{\pi} + \ln \left(\frac{x}{u_0}\right) \right] \quad (9)$$

It therefore follows from Equations 8 and 9 that, due to the presence of the small crack, the effective failure stress is reduced by an amount $\Delta \sigma_m = -p_c \Delta y_0$ given by the expression

$$\Delta \sigma_m = \left[\frac{2p_c x}{\pi u_0} \left/ \left(1 - \frac{u_0}{\pi}\right) \right. \right] \left\{ 1 + \left[\ln \left(\frac{u_0}{x}\right) \left/ \left(1 - \frac{2u_0}{\pi}\right) \right. \right] \right\} \quad (10)$$

this reduction being with regard to the effective failure stress σ_m , appropriate to the case where there is no crack, i.e. σ_m is given by Equation 7

$$\sigma_m = p_c [1 + \chi + (2\chi + \chi^2)^{1/2}] \quad (11)$$

It should be noted that, in Equations 10 and 11, $x = c/h$, $\chi = v_c E_0 / 2\pi p_c h$ while u_0 is given by Equation 6.

Equation 10, coupled with Equation 6 for u_0 , allows the reduction $\Delta\sigma_m$ in the effective failure stress due to the presence of a small crack of depth $c = xh$ to be determined in terms of the parameter $\chi = v_c E_0 / 2\pi p_c h$. Now h is a length parameter, and is a measure of the ‘‘applied’’ stress gradient. In earlier work [5] dealing with failure caused by the formation of a cohesive zone at a blunt stress concentration, it was shown how the effective failure stress can be estimated by using the planar surface methodology of this section and inputting the appropriate value of h which, in the blunt stress concentration case, is a measure of the stress gradient ahead of the stress concentration. In the next section we show how this section’s methodology can be used to assess the effect of a small crack, in the surface of a blunt stress concentration, on the reduction in the effective failure stress associated with failure at an uncracked blunt stress concentration.

4. Cohesive zone formation at a crack in the surface of a blunt stress concentration

Consider the two-dimensional situation where there is a crack of depth c in the surface of a semi-circular cylindrical hole (radius d) which is in the planar surface of a semi-infinite solid that is subjected to an applied tensile stress, σ (Fig. 2). There is a cohesive zone, within which the tensile stress is p_c , emanating from the crack tip. The Mode III analogue of this Mode I situation has been analysed [9], and the exact Mode III results will be applied to the Mode I situation, with the shear modulus replaced by $E_0/2$. The results give the effective stress $\sigma_{m^*}(c)$ that the solid is able to sustain, i.e. the stress required to induce a displacement v_c at the crack tip. ($\sigma_{m^*}(c)$ is the elastically calculated stress at the flaw surface assuming there to be no crack and no cohesive zone, and is a half of the applied stress needed for failure because the stress concentration factor associated with the hole is 2 with Mode III loading.) The results [9] can be represented in the following form

$$v_* = \frac{\sigma_{m^*}(c)}{p_c} = \frac{2}{\pi} \cos^{-1} \left(\frac{p_*}{q_*} \right) + \frac{2}{\pi} \cos^{-1} \left(\frac{1 + p_*^2}{1 + q_*^2} \right)^{1/2} \quad (12)$$

$$\frac{\pi^2 \chi_*}{4} = \frac{\pi E_0 v_c}{8 p_c d} = (1 + p_*^2)^{1/2} \ln \left(\frac{1 + q_*^2}{1 + p_*^2} \right)^{1/2} + p_* \ln \left(\frac{q_*}{p_*} \right) \quad (13)$$

$$p_* = \frac{x_*}{(1 + x_*)} \left(1 + \frac{x_*}{2} \right) \quad (14)$$

with $x_* = c/d$ and where q_* is a parameter greater than p_* .

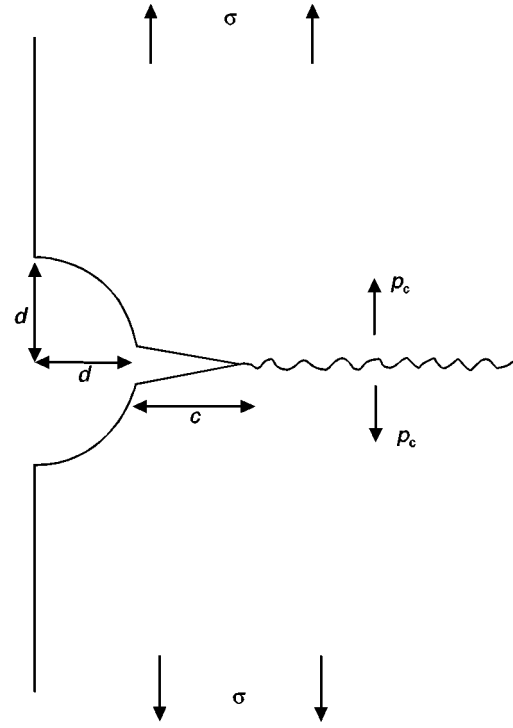


Figure 2 The model of a cohesive zone emanating from the tip of a crack in the surface of a semi-circular cylindrical hole which is in the planar surface of a semi-infinite solid.

We are concerned with the effect of a small crack, i.e. $x_* = c/d$ is small, and how this reduces the effective failure stress below the value $\sigma_{m^*}(0) \equiv \sigma_{m^*}$ appropriate to the case where there is no crack. Thus, we are interested in the situation where χ_* is finite and where $x_* = c/d$ is small. Now, in the limiting case where there is no crack, i.e. $x_* = 0$, let $q_* = q_{*0}$ and $y_* = y_{*0}$, whereupon Equations 12–14 give, for this special case

$$q_{*0} = \left[\exp \left(\frac{\pi^2 \chi_*}{2} \right) - 1 \right]^{1/2} \quad (15)$$

and

$$y_{*0} = 1 + \frac{2}{\pi} \sec^{-1} \exp \left(\frac{\pi^2 \chi_*}{4} \right) \quad (16)$$

Equation 16 being in accord with that obtained in the earlier work [5].

Now, when x_* is small and χ_* is finite, let $q_* = q_{*0} + \Delta q_{*0}$ and $y_* = y_{*0} + \Delta y_{*0}$ where Δq_{*0} and Δy_{*0} are both small. Then, to the first order in small quantities, Equations 12–14 give

$$\Delta y_{*0} = \frac{2}{\pi} \left[-\frac{x_*}{q_{*0}} + \frac{\Delta q_{*0}}{(1 + q_{*0}^2)} \right] \quad (17)$$

and

$$\frac{\Delta q_{*0}}{(1 + q_{*0}^2)} = \frac{x_*}{q_{*0}} \ln \left(\frac{x_*}{q_{*0}} \right) \quad (18)$$

It therefore follows from Equations 17 and 18 that, due to the presence of the small crack, the effective

failure stress is reduced by an amount $\Delta\sigma_{m^*} = -p_c\Delta y_{*0}$ given by the expression

$$\Delta\sigma_{m^*} = \frac{2p_c}{\pi} \frac{x_*}{q_{*0}} \left[1 + \ln\left(\frac{q_{*0}}{x_*}\right) \right] \quad (19)$$

this reduction being with regard to the effective failure stress σ_{m^*} appropriate to the case where there is no crack, i.e. σ_{m^*} is given by equation 16 as

$$\sigma_{m^*} = p_c \left[1 + \frac{2}{\pi} \sec^{-1} \exp\left(\frac{\pi^2 x_*}{4}\right) \right] \quad (20)$$

It should be noted that, in Equations 19 and 20, $x_* = c/d$, and $\chi_* = v_c E_0 / 2\pi p_c d$. Equation 19 coupled with Equation 15 for q_{*0} , allows the reduction $\Delta\sigma_{m^*}$ in the effective failure stress due to the presence of a small crack of depth $c = x_* d$ to be determined in terms of the parameter $\chi_* = E_0 v_c / 2\pi p_c d$ where d is the hole radius. This reduction is with regard to the effective failure stress σ_{m^*} (given by Equation 20) appropriate to the case where there is no crack, and the cohesive zone forms directly at the hole surface.

We now show how the planar surface methodology formulated in the preceding section gives results that are consistent with those obtained in this section. In the preceding section we considered the case of a cohesive zone emanating from a crack in the surface of a semi-infinite solid which is subjected to a linear stress gradient manifested by the parameter h . Now, with this section's model (Mode III), h is, in fact, equal to the hole radius d [10] and consequently χ_* is equivalent to χ . Because we are dealing with only a linear stress distribution, we would expect that if there is accord between the planar surface methodology's predictions and the results of this section, then this accord should be for the case where the zone size is small so that it is confined to the linear stress range. That this is the case is readily seen, for with $\chi_* = \chi$ then being small, σ_m as given by Equation 11 is equivalent to σ_{m^*} as given by Equation 20, i.e.

$$\sigma_m = \sigma_{m^*} = p_c [1 + (2\chi)^{1/2}] \quad (21)$$

to the first two terms in increasing powers of χ . Furthermore, $\Delta\sigma_m$ as given by Equation 10 is equivalent to $\Delta\sigma_{m^*}$ as given by Equation 19, i.e.

$$\Delta\sigma_m = \Delta\sigma_{m^*} = \frac{2p_c}{\pi} \frac{x2^{1/2}}{\pi\chi^{1/2}} \left[1 + \ln\left(\frac{\pi\chi^{1/2}}{x2^{1/2}}\right) \right] \quad (22)$$

with $x = c/d = c/h$. We have accordingly demonstrated how the planar surface methodology can be used to quantify cohesive zone formation in the vicinity of a blunt flaw (with or without a crack in its surface), by inputting the appropriate value of h in the planar surface methodology, with h being a measure of the linear stress gradient ahead of the flaw surface.

5. Discussion

The paper has proceeded from the basis that the maximum load size effect for a brittle structure is deterministic, and is associated with the formation of a damage region. By modelling this damage in terms of the cohesive zone description, and by associating

the maximum load with the attainment of an elastically calculated effective failure stress at the free surface from which a zone emanates, earlier work [4, 5] has shown that the effective stress is critically dependent on the applied loading-induced stress gradient beneath the surface, with the effective failure stress increasing with the steepness of the stress gradient. The present work has extended the earlier considerations by assessing the effect of a small surface crack on the effective failure stress, with Mode III exact solutions being used to quantify the more practical Mode I conditions that usually exist in service. There is scope for performing actual Mode I analyses for the small flaw situation, as has been done for the Mode I planar surface situation [5], but this will probably involve numerical procedures.

Expressions have been obtained for the reduction in effective failure stress for the cases where (a) there is a crack in the surface of a semi-infinite solid that is subjected to a linear driving stress gradient, and (b) there is a crack in the surface of a semi-circular cylindrical hole in the surface of a semi-infinite solid that is subjected to an applied tensile stress. Furthermore, it has been demonstrated how the results for these two situations relate to each other.

To put the results obtained here in perspective, let us take the planar surface situation results and apply them to the bent specimen geometry. If the cohesive zone size at failure is not unduly large, we can use the small χ results, when the effective failure stress σ_m in the absence of a crack is given by Equation 21, while the reduction in effective failure stress, $\Delta\sigma_m$, is given by Equation 22. Consequently, the reduction in effective failure stress due to the presence of a crack in the tensile surface is given by the expression

$$\frac{\Delta\sigma_m}{\sigma_m} = \frac{2}{\pi} \frac{x2^{1/2}}{\pi\chi^{1/2}} \left[1 + \ln\left(\frac{\pi\chi^{1/2}}{x2^{1/2}}\right) \right] / [1 + (2\chi)^{1/2}] \quad (23)$$

where $\chi = v_c E_0 / 2\pi p_c h$ and $x = c/h$; c is the crack depth and h is a measure of the stress gradient and can be equated with $w/2$ where w is the beam depth. Thus, for an ordinary concrete with, say, the specific fracture energy $G_F = 100 \text{ N m}^{-1}$ (G_F is equal to $p_c v_c$ with the constant stress cohesive zone representation), $p_c = 3 \text{ MPa}$, $E_0 = 30 \text{ GPa}$, and with a beam depth of 1 m, we see that $x \sim 0.1$. Hence with $c = 2 \text{ cm}$ whereupon $x = c/h = 0.04$, we see from Equation 23 that the fractional reduction in the effective failure stress due to the presence of the crack is 10%. As regards general behaviour trends, we see that the fractional reduction for a fixed h increases (obviously) as the crack depth increases and as χ decreases, i.e. as the specific fracture energy G_F decreases and the cohesive zone stress p_c increases.

6. Conclusion

The paper has assessed the effect of a small surface flaw on the effective failure stress of a brittle structure, and has shown how the small flaw tolerance depends on the stress gradient beneath the surface, flaw depth and material fracture properties.

References

1. J. OZBOLT and R. ELIGEHAUSEN, in "Size-Scale Effects in the Failure Mechanisms of Materials and Structures", edited by Alberto Carpinteri (Spon, London, 1996) p. 290.
2. M. ELICES, G. V. GUINEA and J. PLANAS, *ibid.*, p. 309.
3. Y. N. LI and Z. P. BAZANT, *ibid.*, p. 274.
4. E. SMITH, *J. Mater. Sci.* **32** (1997) 3939.
5. E. SMITH, *J. Mater. Sci.* **33** (1998) 29.
6. D. S. DUGDALE, *J. Mech. Phys. Solids* **8** (1960) 100.
7. B. A. BILBY, A. H. COTTRELL and K. H. SWINDEN, *Proc. R. Soc.* **A272** (1963) 304.
8. H. TADA, P. C. PARIS and G. R. IRWIN, "The Stress Analysis of Cracks Handbook", Del Research Corporation, Hellertown, PA, (1973).
9. B. A. BILBY and P. T. HEALD, "*Proc. R. Soc.*" **A305** (1968) 429.
10. E. SMITH, *Int. J. Eng. Sci.* **6** (1968) 129.

*Received 4 December 1997
and accepted 15 May 1998*